Contents

Supplemental Methods and Materials

T-bet DBD construct. Mus musculus T-bet DNA binding domain (T-bet DBD) corresponding to residues 135-326 of full length mouse T-bet was cloned into the pQE30 vector (Qiagen) using the BamHI and Hind III restriction sites to yield the N-terminal His-tagged T-bet DBD construct, T-bet-DBD-pQE30.

Expression and purification of T-bet. E. coli BL21-DE3 or C43-DE3 cells transformed with the T-bet-DBD-pQE30 vector were grown in LB supplemented with 100 μg/mL ampicillin to an OD_{600} of ~0.6 at 37 °C prior to induction of protein expression with IPTG at a final concentration of 0.5 mM. After induction, the cells were grown overnight at 20°C with agitation at 250 rpm, harvested after centrifugation for 10 minutes at 5000 rpm in a F10-6x500y rotor (Thermo Scientific), (Piramoon Technologies), and stored frozen at -80 °C until further purification.

Cell pellets typical from a 3-liter culture were thawed and resuspended in 150 mL of 20 mM HEPES, pH 7.5, 5 mM KCl, 1 M NaCl, 0.1 mM PMSF, 1 mM arginine, 1 mM glutamine, and 5% sucrose. The resuspended cells were ruptured by two cycles of thaw/freeze followed by sonication. The lysate was immediately centrifuged at 13000 rpm in a Beckman Coulter JA-20 rotor for 1 hour. The supernatant from the centrifugation was loaded into an 8-mL Talon resin column equilibrated in 20mM HEPES, pH 7.5, 5 mM KCl, 1 M NaCl, and 5% sucrose (equilibration buffer). T-bet DBD was eluted with a linear gradient of imidazole (0 mM to 500 mM). The peak containing the T-bet DBD was concentrated and loaded into a HiPrep Sephacryl HR S200 size exclusion column (GE Healthcare) which was pre-equilibrated in equilibration buffer at a rate of 0.3 mL min^{-1}. Purified T-bet from the size exclusion column was concentrated to ~10-35 mg/mL and stored at -80 °C.

Crystallization of T-bet-DNA complex. T-bet DBD was crystallized in complex with a 24 base pair palindromic deoxyribonucleic acid oligomer (5'-AATTTCACACCT AGGTGTGAAATT). The palindromic DNA was dissolved in 10 mM Tris and 1 mM EDTA to a final concentration of 5mM and annealed by heating the sample to 100°C in a water bath and allowing the sample to passively cool to ambient temperature.

In a typical crystallization experiment, a 50 μL aliquot of ~33 mg/mL T-bet was thawed and mixed with 1.2 fold molar excess of annealed oligonucleotide. The T-bet/DNA sample was exchanged into 20mM HEPES, pH 7.5, 5 mM KCl, 300 mM NaCl, and 1 mM DTT by dilution and concentrated using an Amicon Ultra 3K concentration unit (Millipore).

The T-bet-DNA complex was crystallized by the hanging drop method using Hampton Research VDX 24-well plates. Typically, 2ul of T-bet/DNA sample mixed with 2ul of 85 mM sodium citrate, pH 5.1, 1.7 M sodium formate, and 15% ethylene glycol was sealed over a well containing 1 mL of mother liquor. Crystal formation was apparent after 1-3 days of incubation at 20 °C.

Crystallographic data collection and structure determination. We initially collected data on native T-bet crystals on our home source Bruker UltraStar and later at beamline 23-ID or 19-ID of the Advanced Photon Source at Argonne National Laboratory. The X-ray wavelength was set at 0.98 Å. We cryo-cooled T-bet crystals in liquid nitrogen after

a 1-2 second wash in fresh mother liquor. Diffraction data were collected at 100 K on a Mar225 CCD detector (MarUSA) and processed with the program HKL2000 (1). The crystals belonged to the space group $P6_1$ with two molecules of T-bet–DNA complex per asymmetric unit. For the native data, we combined data collected from 2 different crystals to obtain both the extreme low and high resolution reflections. A homology model of the T-bet DBD monomer was constructed from the sequence of the DNA binding domain (residues 135-326) of Mus musculus T-bet (NCBI Protein code: 187953773) and the crystal structure of the Xenopus laevis Brachyury T-domain (Protein Data Bank code: 1XBR) using the online server Swiss-Model (2). The homology model and a model of ideal B-form DNA were used sequentially as molecular-replacement search models and yielded a solution with the program Phaser (3).

All possible hexagonal space-groups were tried; the cleanest solution was obtained in $P6_1$. It was possible to rule out a number of solutions based on the fact that the DNA strands had to be oriented parallel to the z-axis of the crystal. This fact was established early in the structure determination by inspection of the diffraction pattern: it contained a strong “meridional” fiber-diffraction streak at the same 3.4 Å spacing originally observed by Rosalind Franklin for B-form DNA, indicating the direction of the double helical axis (“SI Appendix, Fig. S1”).

After multiple rounds of maximum likelihood, rigid body, TLS refinement using PHENIX (4), and simulated annealing refinement, the R-factor was lowered to 0.28 with an R_{free} of 0.34. A 2Fobs-Fcalc map following rigid body refinement showed reasonable electron density for ~70% of the model (“SI Appendix, Fig. S2”). To improve definition of the electron density, we performed B-factor sharpening with CNS (5). Cycles of rebuilding and refinement were carried out using the programs Coot (6) and PHENIX (4), and gradually led to a model for the entire structure. In the final round of refinement, TLS refinement was carried out using a total of 4 TLS groups (7). The current Rcryst and Rfree are 26% and 30%, respectively (RMSD from ideal bond lengths and angles are 0.004 Å and 0.9°, respectively). Complete data collection and refinement statistics are given in “SI Appendix, Supplemental Table S1.”

Size exclusion chromatography. SEC measurements were carried out using a YMC-Pack Diol-120 Size Exclusion Chromatography Column. Molecular weight standards used were blue dextran (MW 2,000,000), albumin (MW 67,000), ovalbumin (MW 45,000), chymotrypsinogen (MW 25,000) and ribonuclease A (MW 13,700). The standards gave an excellent linear fit of elution time vs molecular weight (R^2 = 0.9381). Purified T-bet DNA binding domain applied to this column eluted in two peaks with retention times corresponding to molecular weights 22,707 and 42,838 as expected for a mixture of monomer and homodimer.

Fluorescence DNA binding assays. All fluorescence measurements were carried out using the Hitachi F-2500 Fluorescence Spectrophotometer at 25 ^{o}C. The buffer used for all fluorescence measurements was 20 mM MES, pH 6.0, 300 mM NaCl, 5 mM KCl, 100 nM BSA, 0.003% Brij 35, and 1 mM DTT.

FRET DNA binding assay. HPLC purified 3'-FAM labeled and 3'-TAMRA labeled 5'-AATTTCACACCT AGGTGTGAAATT DNA were ordered from Eurofins MWG/Operon. Both these labeled DNAs were solublized in 10 mM Tris, pH 7.5, and 1 mM EDTA to a

concentration of 100 μM and independently annealed by heating the samples to 60^{o}C in a water bath and allowed to cool passively to ambient temperature.

FRET efficiency (E) was calculated with the equation, $E = 1 – (F_{DA} / F_D)$, where F_{DA} is the relative fluorescence intensity of the donor DNA (3'-FAM- labeled DNA) in the presence of acceptor DNA (3'-TAMRA- labeled DNA) and F_D is the relative fluorescence intensity of the donor DNA in the absence of acceptor DNA. The excitation and emission wavelengths used to measure the fluorescence of the donor DNA were 483 nm and 521 nm respectively.

Fluorescence Intensity DNA binding assay. The non-FRET decrease quenching ofin the fluorescence intensity of 3'-TAMRA- labeled dsDNA fluorescence upon binding to T-bet DBD was used to measure the DNA dissociation constant ($K_{d(DNA)}$). In a typical assay, 1 nM 3'-TAMRA- labeled dsDNA was titrated with increasing concentration of T-bet DBD. The resulting titration curve was fitted to the equation, $F = (F_{min} * Tbet) / (K_d + Tbet)$, where F is the fluorescence intensity, F_{min} is the minimum fluorescence intensity, Tbet is the T-bet DBD concentration, and K_d is the dissociation constant for DNA.

DNA dissociation kinetics assay. Dissociation kinetics of T-bet from DNA were monitored by observing the change in fluorescence of 3'-FAM- dsDNA (ex 483 nm, em 521 nm) and 3'-TAMRA- dsDNA (ex 568 nm, em 581 nm) over time following the dilution of T-bet/DNA complex and addition of excess unlabeled DNA. Typically, 500 nM T-bet DBD, 250 nM 3'-TAMRA- dsDNA, and 250 nM 3'-FAM- dsDNA in assay buffer were diluted 40-fold into buffer containing 16000-fold excess unlabeled dsDNA. The change in fluorescence of 3'-FAM- dsDNA and 3'-TAMRA- dsDNA were monitored over a period of ~1 hour. The dissociating rates of DNA from the quaternary T-bet/DNA complex off rates were calculated from the data fitted to either a one-phase exponential decay function or a two-phase exponential decay function.

CD4$^+$ T helper differentiation in vitro. Mouse *Tbx21*$^{-/-}$ and wild-type (C57BL/6) CD4$^+$ T cells were stimulated for 48 hours with soluble anti-CD3 antibody (2 μg/mL; clone 145-2C11; eBioscience) in the presence of irradiated splenocytes (2000 rads) at a ratio of 5:1. CD4$^+$ T cells were cultured in RPMI complete media (RPMI, 10% FBS, 10 mM HEPES, 10 mM L-glutamine, 10 mM sodium pyruvate, 10 mM non-essential amino acids, and 50 μM β-mercaptoethanol) and differentiated into T_H1 cells in the presence of hIL-2 (200 U/mL; National Cancer Institute Biological Resources Branch Preclinical Repository), mIL-12 (10 ng/mL; Peprotech) and anti-mIL-4 antibody (10 μg/mL; clone 11B11; BioXCell) for 5 days. Fully differentiated T_H1 cells were re-suspended at $2x10^6$/mL and activated in the presence of 50 ng/ml PMA and 1 μM ionomycin (PMA/I) for 5 hours before formaldehyde crosslinking for the *in vivo* 3C assay.

In vivo Chromosome Conformation Capture (3C) assay. Using the *in vivo* 3C assay, long range DNA looping interactions within the mouse interferon-γ gene locus were probed in T-bet negative T_H1 helper cells and in T-bet positive T_H1 helper cells derived from Tbx21$^{-/-}$ and wild-type mice (C57BL/6) respectively. The 3C assay was performed using restriction enzyme BglII. Unless noted otherwise, the 3C protocol used was essentially as previously described (8,9). PCR products were visualized and quantified with SYBR Green (Invitrogen) using a fluorescence imager (Molecular Devices Typhoon 8600). The control library was generated using BAC clone RP24-348O11 (Children's Hospital Oakland Research Institute). To allow direct data comparison between the two

3C samples, 3C profiles were normalized using 15 interaction frequencies measured within a conserved gene desert region (chr3:147095578-147225578), the actin gene (chr19:34314493-34330493), and the GAPDH gene (chr6:125111899-125117399). Primer sequences used in the 3C assay are shown in "SI Appendix, Supplemental Table S2."

In vitro Chromsome Conformation Capture (3C) assay. Long-range DNA looping interactions induced by the T-bet DBD within the interferon-γ gene locus were probed using a novel *in vitro* 3C assay. T-bet DBD and purified naked DNA containing the interferon-γ gene locus (Bacterial Artificial Chromosome RP24-348O11) were incubated together. Long-range DNA looping interactions induced by the addition of T-bet was detected by the original 3C method. Unless noted otherwise, the 3C protocol was essentially as described for the *in vivo* 3C assay. In a typical *in vitro* 3C experiment, 48 ng/µl RP24-348O11 BAC DNA was incubated with 0.95 µM T-bet DBD in buffer containing 50mM Tris-HCl, pH 7.9, 100 mM NaCl, 10 mM $MgCl_2$, 1 mM DTT, and 100 µg/mL BSA (NEB3 + BSA buffer). After 30 minutes on ice, the sample was crosslinked as described previously (Miele and Dekker, 2009) and unbound proteins were removed using a DNA cleaning kit from Zymo Research (DNA Clean & Concentrator™ Kit). The purified cross-linked DNA (289 ng; ~1.45 ng/µl) was digested overnight at 37^{o}C with 100 units of BglII (New England Biolabs) in NEB3 + BSA buffer. Following digestion, the sample was cleaned and ligated with 10 units of T4 DNA ligase (Invitrogen) for 2 hours at 16^{o}C at a final DNA concentration of 10 pg/µL in ligation buffer containing 50 mM Tris-HCl, pH 7.5, 10 mM $MgCl_2$, 10 mM DTT, and 1 mM ATP. The ligated DNA products were concentrated using Amicon Ultra 30K filtration units (Millipore) and purified with the DNA cleaning kit following formaldehyde crosslink reversal and proteinase K treatment as described previously (9). As a T-bet negative control, a separate 3C sample was processed replacing T-bet with an equivalent amount of BSA. Looping interactions were probed by PCR using 92.3 pg/µl 3C DNA template per reaction. Primers used to probe looping interactions were the same as those used in the *in vivo* 3C assay.

Supplemental References

1. Otwinowski Z, Minor W (1997) Processing of X-ray diffraction data collected in oscillation mode. *Methods Enzymol* 276:307-326.

2. Schwede T, Kopp J, Guex N, Peitsch MC (2003) SWISS-MODEL: an automated protein homology-modeling server. *Nucleic Acids Research* 31:3381-3385.

3. McCoy AJ, Grosse-Kunstleve PD, Adams PD, Winn MD, Storoni LC, Read RJ (2007) Phaser crystallographic software. *J. Applied Cryst.* 40:658-674.

4. Adams PD, Afonine PV, Bunkoczi G, Chen VB, Davis IW, Echols N, Headd JJ, Hung LW, Kapral GJ, Grosse-Kunstleve RW, McCoy AJ, Moriarty NW, Oeffner R, Read RJ, Richardson DC, Richardson JS, Terwilliger TC, Zwart PH (2010) PHENIX: a comprehensive Python-based system for macromolecular structure solution. *Acta Cryst* D66:213-221.

5. Brunger AT, Adams PD, Clore GM, Delano WL, Gros P, Grosse-Hunstleve RW, Jiang JS, Huszewski J, Nilges M, Pannu NS, Read RJ, Rice LM, Simonson T, Warren GL (1998) Crystallography & NMR system: A new software system for macromolecular structure determination. *Acta Cryst* D54:905-921.

6. Emsley P, Cowtan K (2004) Coot: model-building tools for molecular graphics. *Acta Cryst* D60:2126-2268.

7. Winn MD, Isupov MN, Murshudov GN (2000) Use of TLS parameters to model anisotropic displacements in macromolecular refinement. *Acta Cryst.* D57:122-133.

8. Dekker J, Rippe K, Dekker M, Kleckner N (2002) Capturing Chromosome Conformation. *Science* 295:1306-1311.

9. Miele A, Dekker J (2009) Mapping *Cis*- and *Trans*- Chromatin Interaction Networks Using Chromosome Conformation Capture (3C). *Methods Mol Biol* 464:105-121.

Supplemental Figures

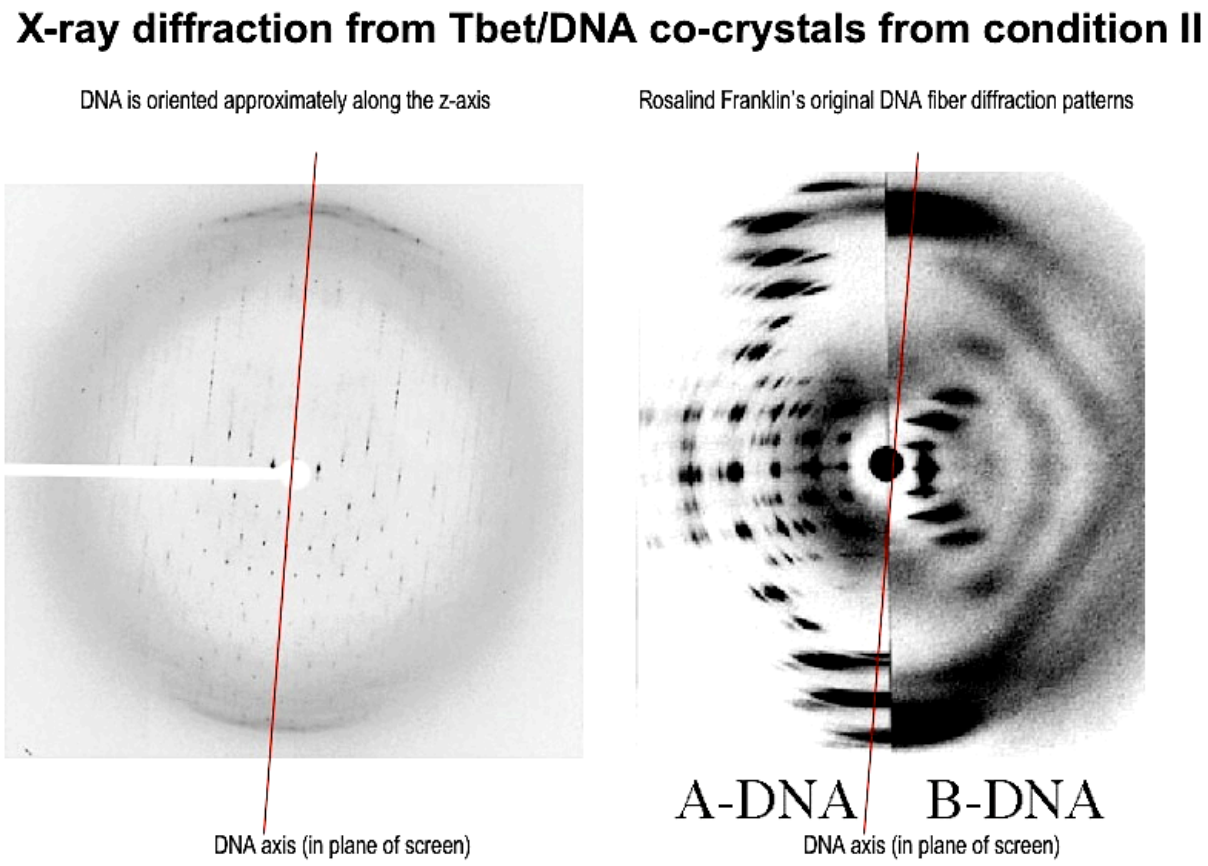

Fig. S1. Section of the T-bet-DNA diffraction pattern showing the lune of diffuse scatter that indicates the orientation of the DNA double helix; shown for comparison are Rosalind Franklin's original X-ray fiber diffraction photos of A-form abd B-form DNA.

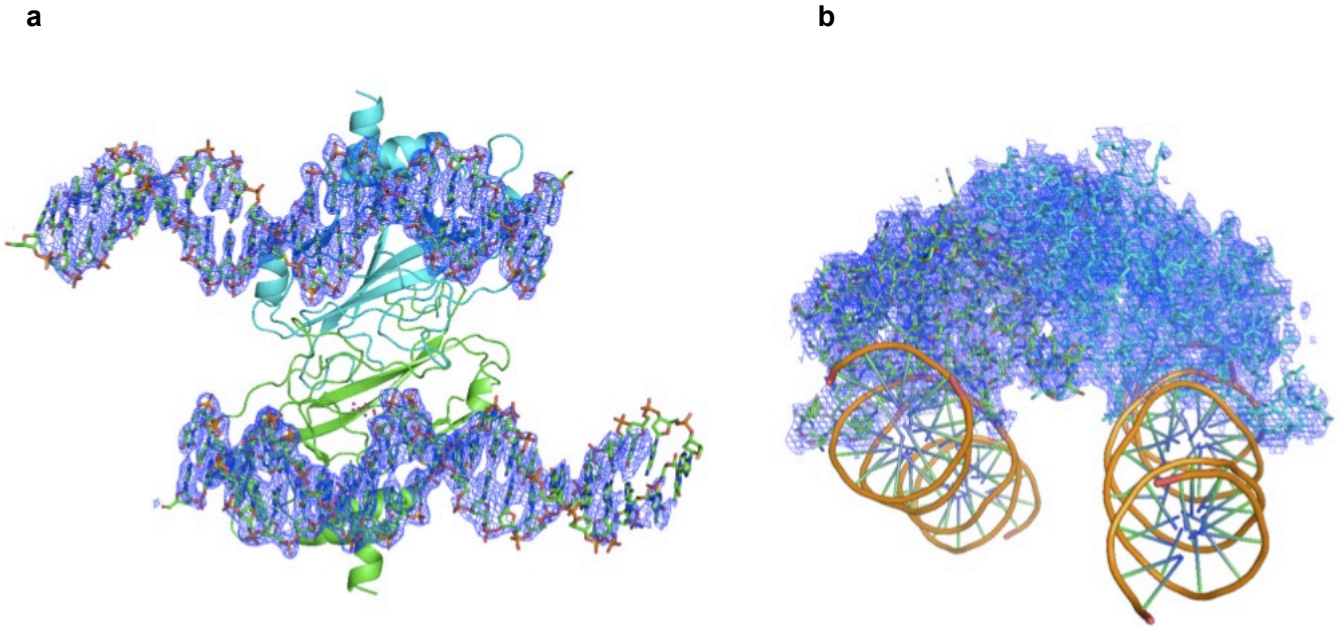

Fig. S2: Initial electron density after molecular replacement and rigid body refinement for the T-bet-DNA complex. The electron density around the DNA (2 sigma level) is shown in (a) on the left; electron density around the T-bet DBD dimer (1 sigma level) is shown on the right in (b).

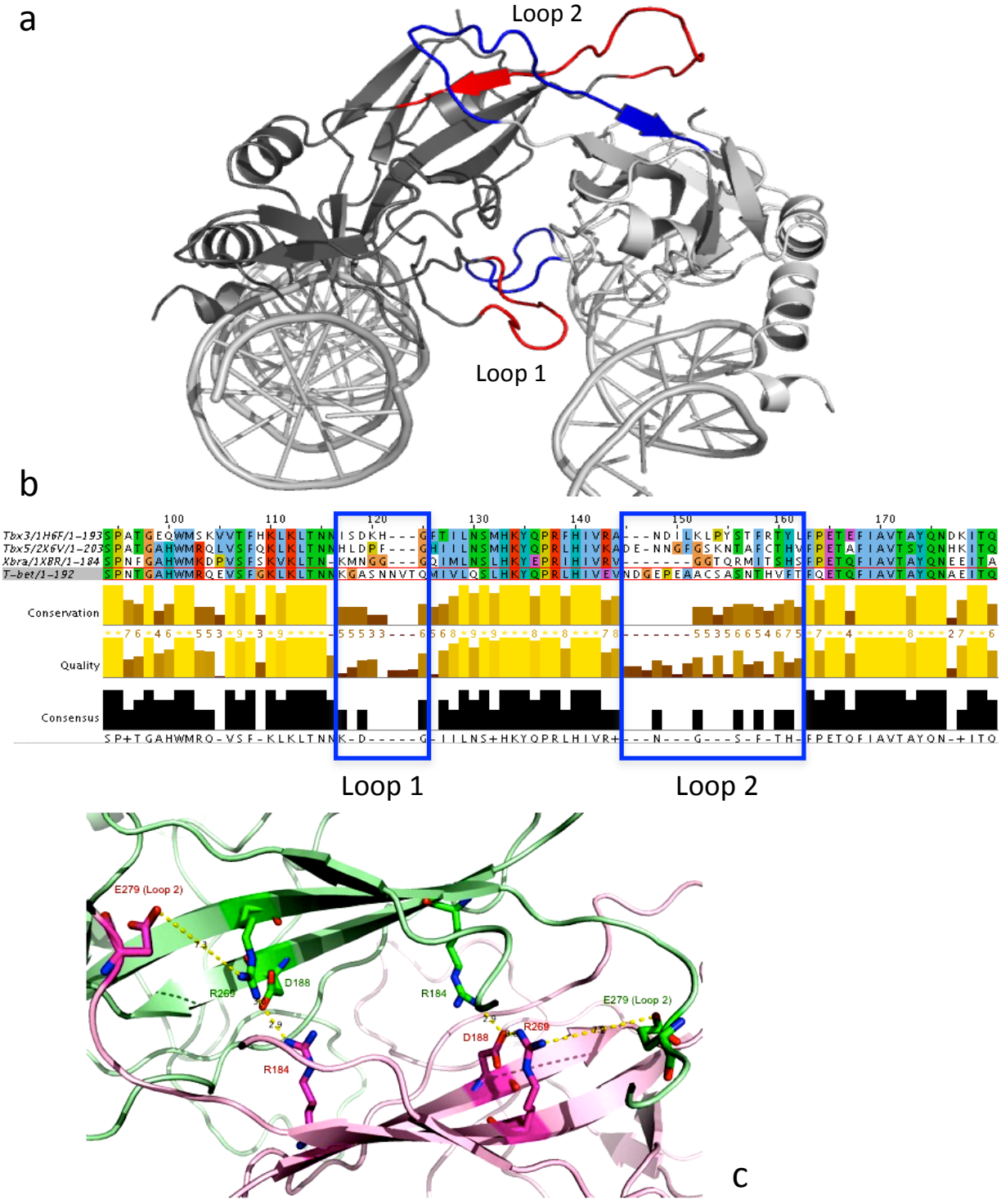

Fig. S3. (a) Structure of the unique T-bet DBD dimer highlighting the two loops that extend out to the adjacent monomer to form a tight, interlocking dimer interface. (b) Sequence alignment of T-bet, Tbx3, Tbx5 and Xbra near the two loops that extend out to form the dimer interface in the T-bet structure. The loop sequences differ in length and sequence in T-bet compared to the other Tbox proteins, and the flanking sequences also show differences. These changes prevent the formation of an Xbra-type dimer and create the novel T-bet dimer interface, which forces the DNA binding sites of the two subunits to be parallel rather than collinear. (c) Close-up of the unique T-bet dimer interface, showing the symmetrical salt bridges and the electrostatic interactions involving Glu 279 from Loop 2.

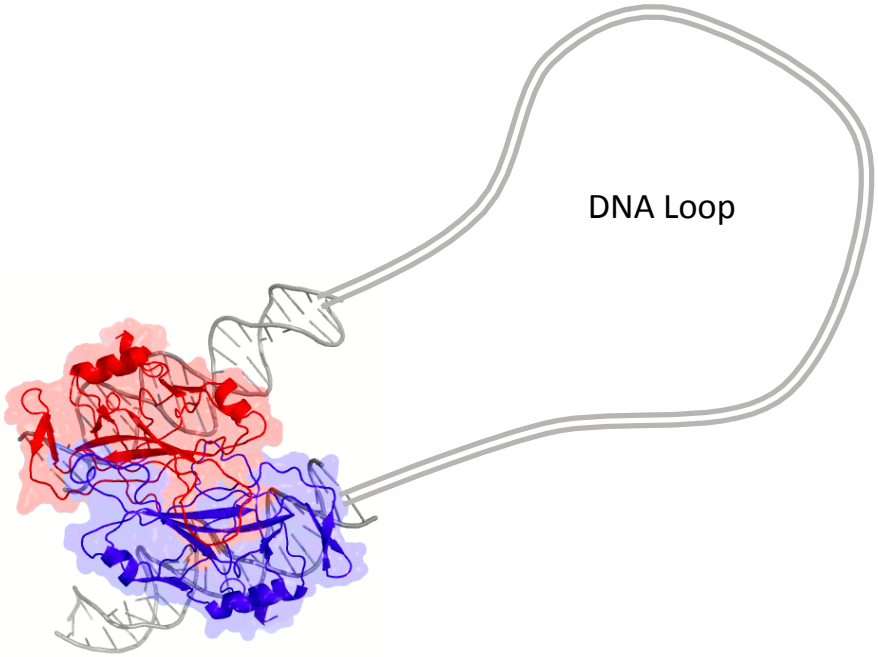

Fig. S4. The two DNA molecules bound to T-bet are continued as cartoons to indicate how T-bet could bind separate sites with an intervening loop of almost any length, or sites on different chromosomes.

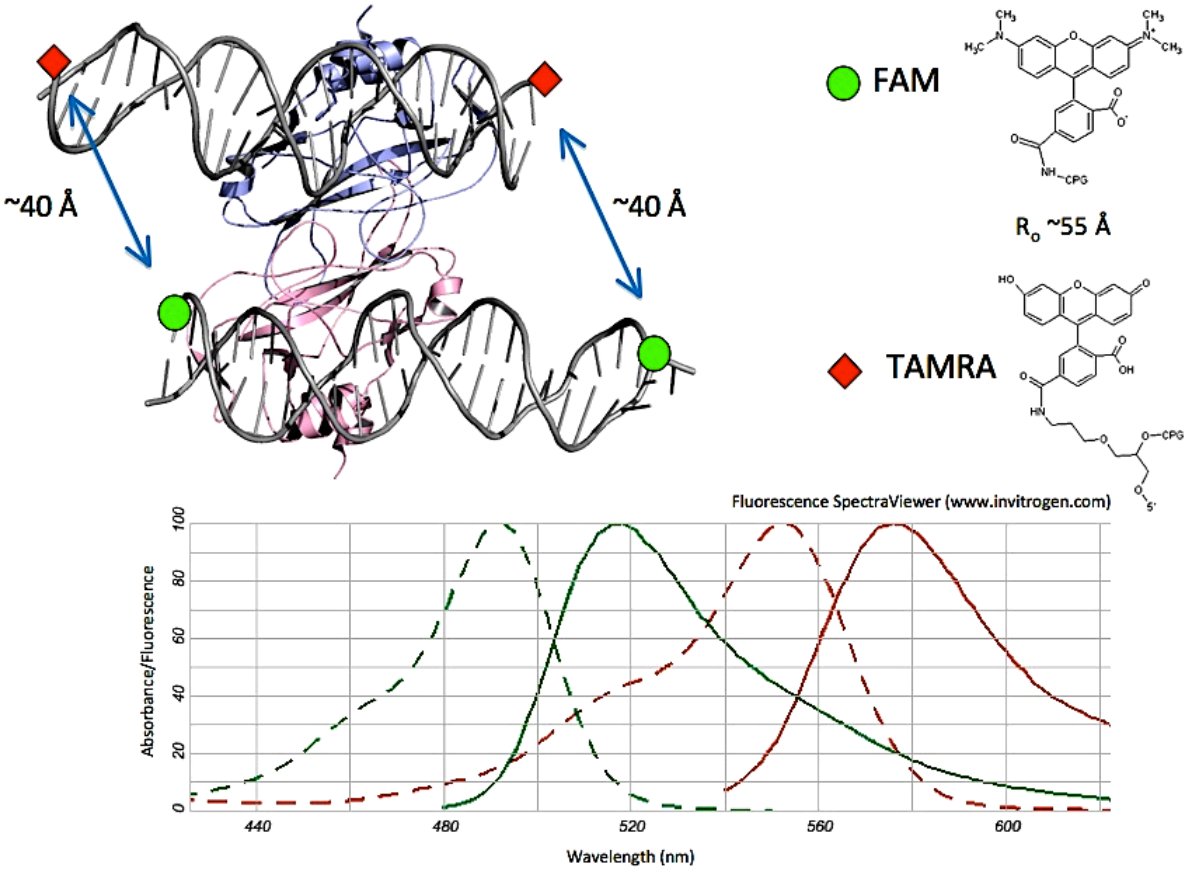

Fig. S5. Design of a fluorescence resonance-energy transfer (FRET) experiment to detect cross-linking of two independent DNA oligomers by T-bet. Two T-bet consensus binding 24-mers were each labeled with a donor fluorophore (FAM) or a acceptor fluorophore (TAMRA), whose donor emission spectra overlaps with the acceptor excitation spectra. The crystal structure predicts a donor-to-acceptor distance of ~40Å if the two different oligomers bind to the same T-bet dimer, which is less than the Forster distance R_o and thus would be expected to produce a strong FRET signal.

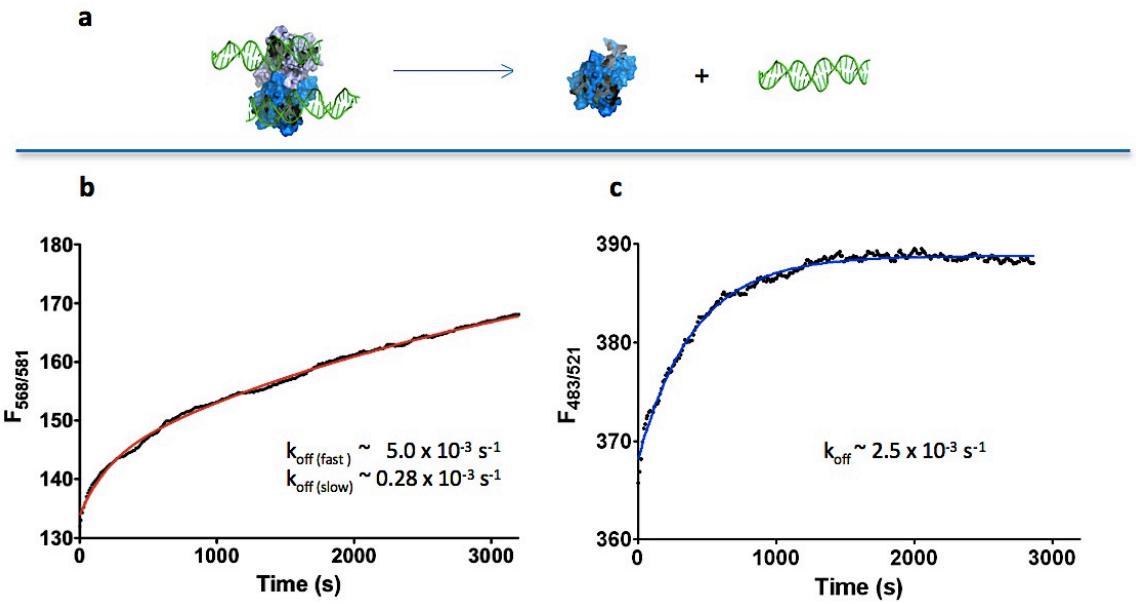

Fig. S6. The dissociation kinetics of T-bet and fluorescently labeled DNA quaternary complex were measured by diluting the preformed quaternary complex into excess unlabeled DNA (a). Two different fluorescence signals were used to observe the dissociation kinetics. The non-FRET TAMRA fluorescence (b) was used to monitor the overall dissociation state of DNA while the FRET FAM fluorescence (c) was used to monitor a subset of dissociation that corresponds to either the dissociation of the first DNA or the dissociation of DNA bound T-bet dimer. The dissociation kinetics were biphasic as detected by the increase in TAMRA fluorescence while monophasic when detected by the increase in FAM fluorescence.

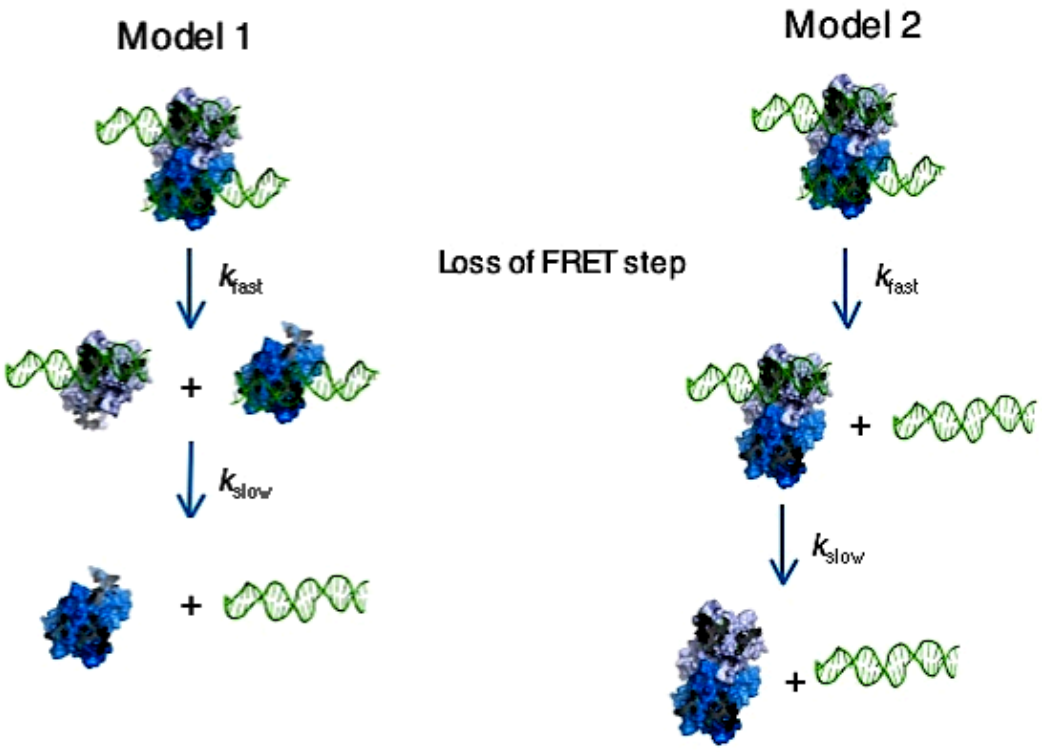

Fig. S7. Two plausible models for the dissociation of DNA from T-bet that are consistent with the dissociation kinetics data shown in Figure S6.

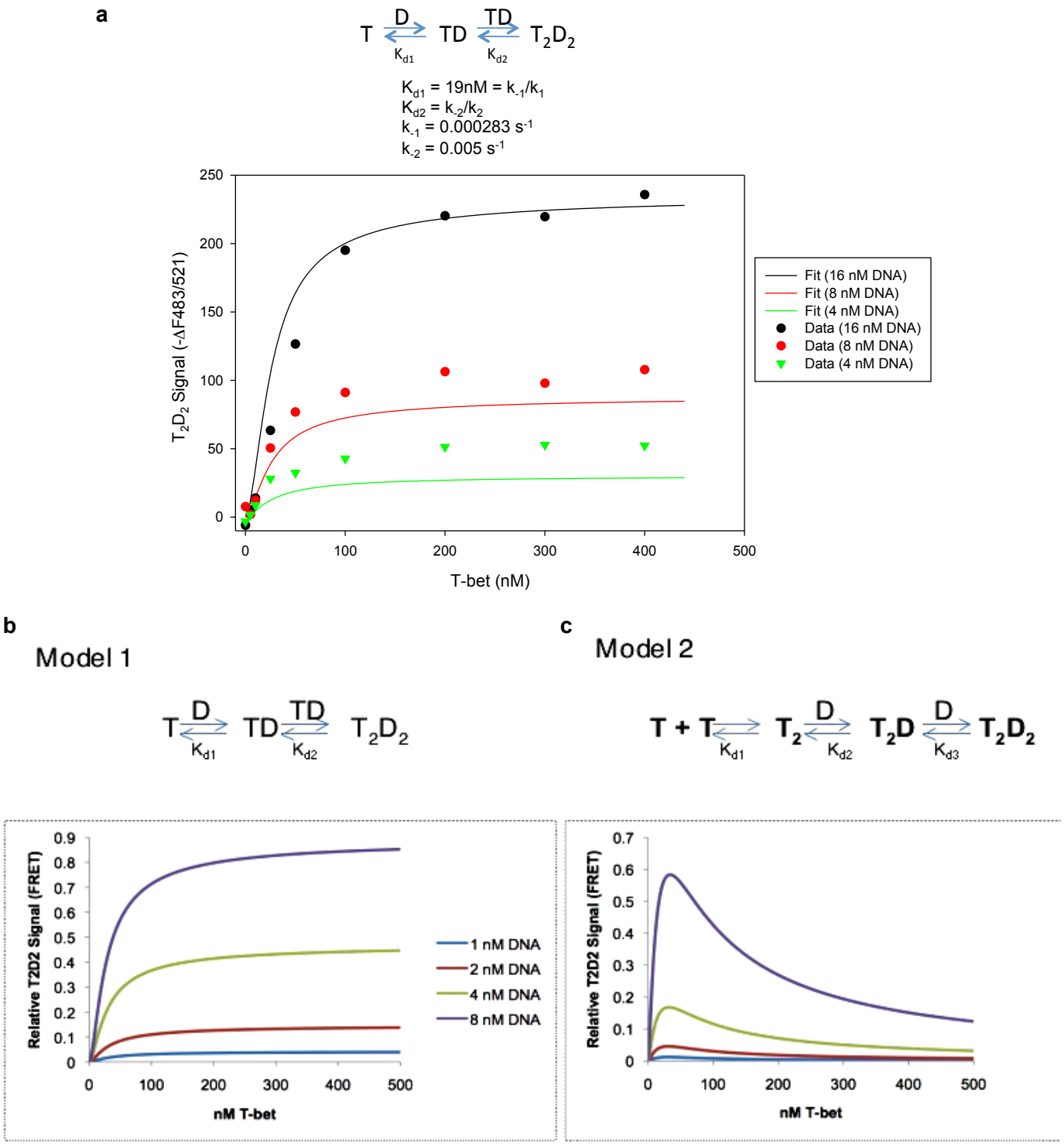

Fig. S8. (a) Predicted concentration dependence for T-bet binding to various concentrations of labeled DNA from Model 1 using binding and dissociation rate constants shown in Figure S6 (solid lines) vs. the observed dependence from FRET measurements (symbols). The fit is best at high DNA concentrations. Predicted dependence of the FRET signal for T-bet binding to labeled DNA as a function of T-bet concentration for various amounts of oligonucleotide for kinetic Model 1 (b) and Model 2 (c). The binding constants used for the simulation were K_{d1} = K_{d2} = 19nM

a

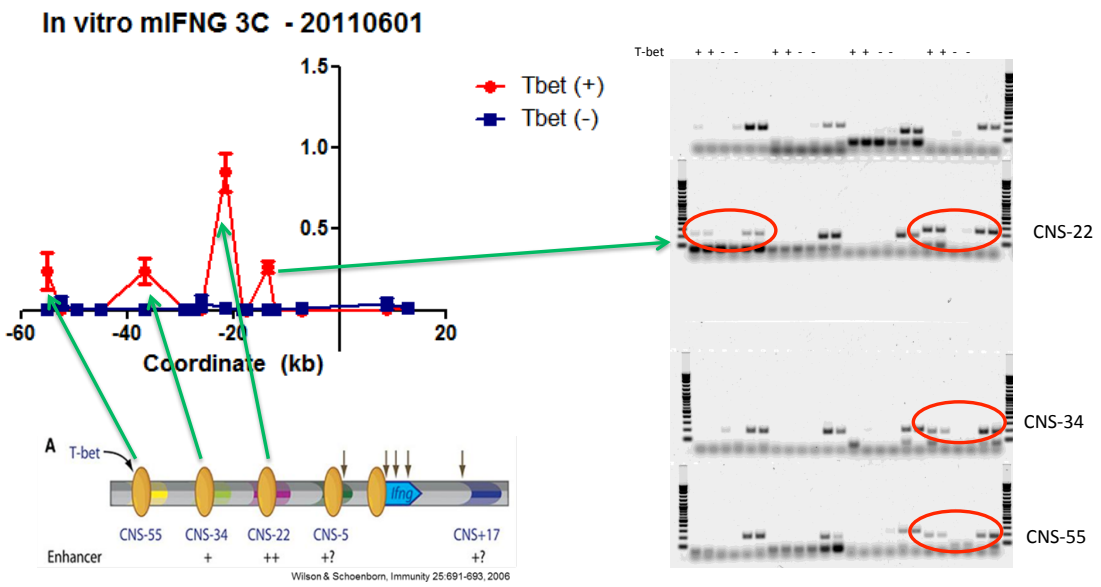

Tbet (+) → 952nM Tbet; ~0.477nM DNA
Tbet (-) → 952nM BSA; ~0.477nM DNA

b

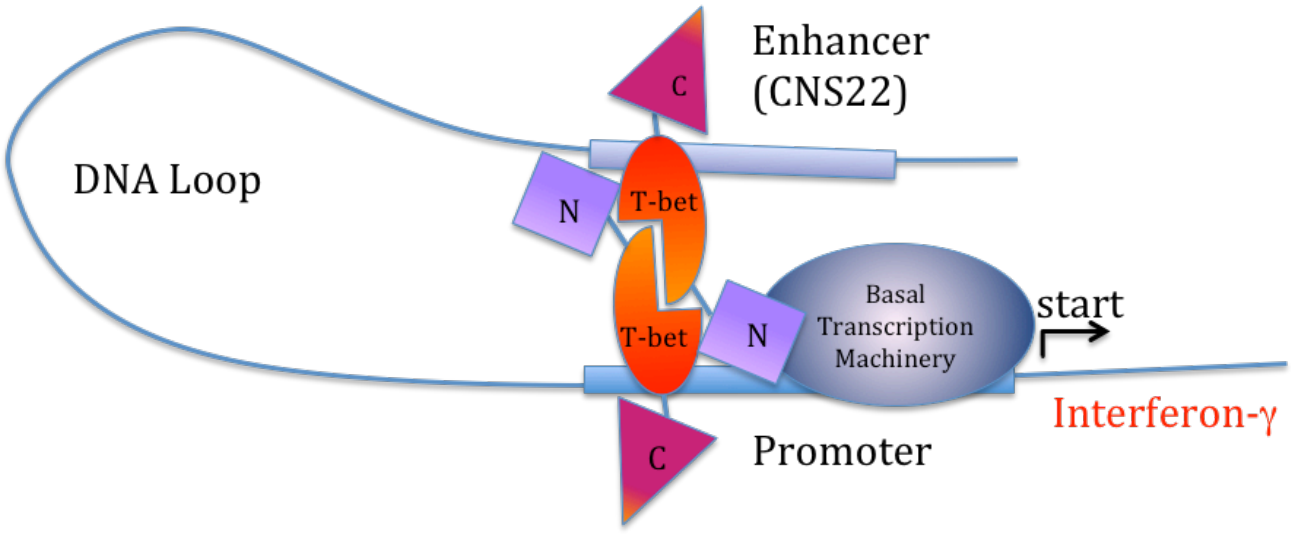

Fig. S9. (a) In vitro C3 data indicating that T-bet is sufficient to bring together the interferon-γ (Ifng) promoter and enhancer sites up to 55kb upstream. (b) A DNA looping model mediated by T-bet that is consistent with the 3C data. For simplicity only the loop formed with the strongest enhancer (CNS-22) is depicted. The N-and C-terminal domains of T-bet are represented, but their precise roles are not determined.

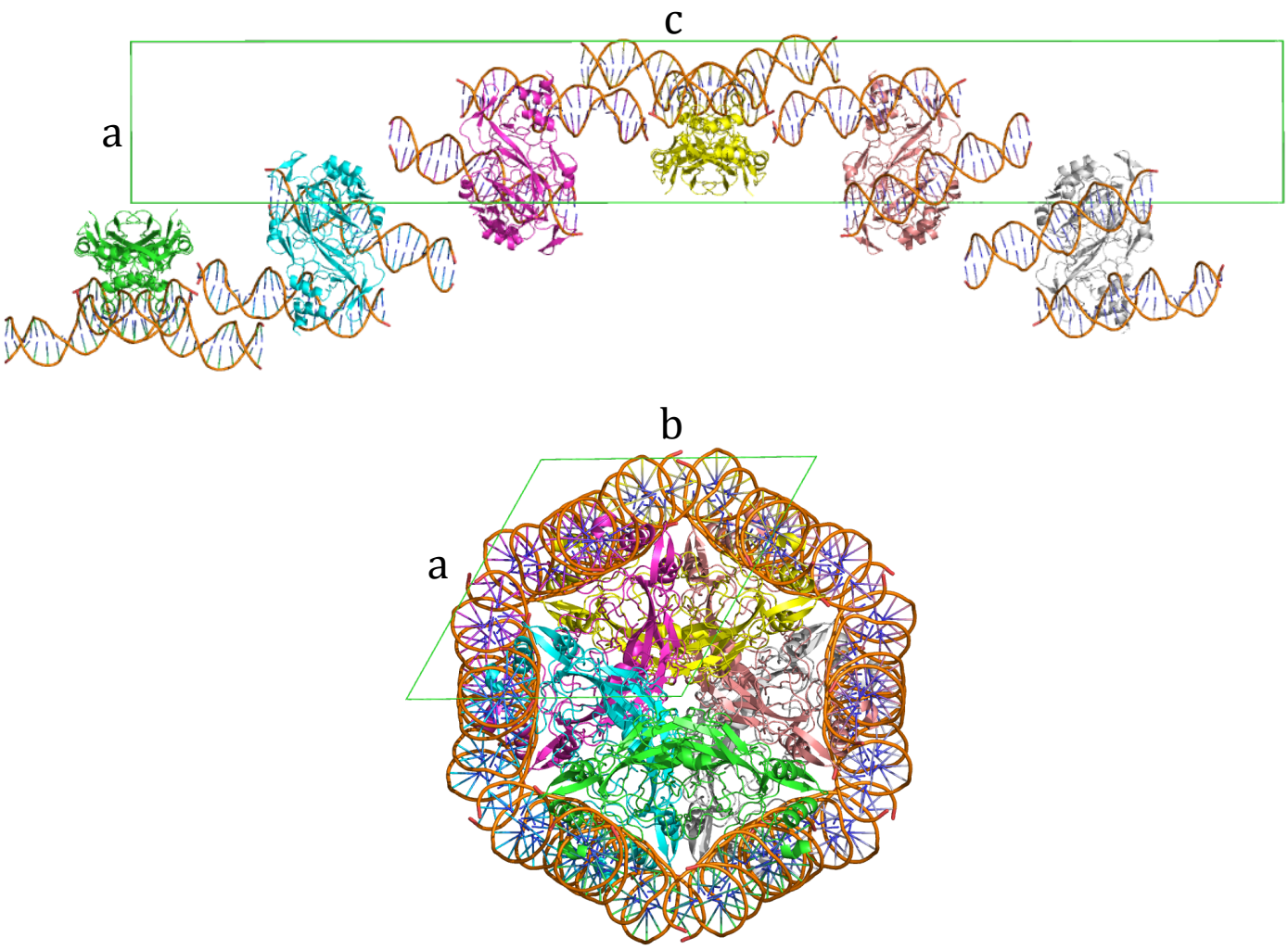

Fig. S10. Crystal packing of T-bet DBD-DNA complex in the asymmetric unit cell.

Supplemental Tables

Supplemental Table S1: Crystallographic data statistics

Data Collection	
Resolution, Å	43.7-2.95
Wavelength, Å	0.97947
Space Group	P61
Unit Cell Dimensions, Å (a, b, c)	70.45, 70.45, 438.4
Unit Cell Angles, ° (α, β, γ)	90, 90, 120
I/σ (last shell)	9.97 (1.62)
R_{sigma} (last shell)	0.0820 (0.8385)
Completeness, % (last shell)	87.9 (41.4)
Number of Reflections	25961
Refinement	
Resolution, Å	43.7-2.95
Number of Reflections	22685
Working	21530
Free	1155
R_{work} (last shell)	0.2588 (0.3002)
R_{free} (last shell)	0.2977 (0.3345)
Structure / Stereochemistry	
Number of Atoms	5062
Solvent	0
Ligands	0
RMSD Bond Length, Å	0.004
RMSD Bond Angles, °	0.866
Protein Data Bank ID	5T1J

Supplemental Table S2. Chromosome Conformation Capture (3C) Primers

Primer Name	Chromosome	Start*	End*	Sequence
mIFNG+3	10	117893036	117893063	CACCTCCAAGATGTGTGACAACCGAGTA
mIFNG+1	10	117888757	117888786	AAATGGATGAGACGGTAGTTCTCAGCCTTC
mIFNG_0.2[$]	10	117884796	117884823	CATGCCTATGAATGACATGGGATGCTGC
mIFNG-1	10	117875534	117875561	ATTTCCAAGCGTAGCAGAATGTGCCATT
mIFNG-2	10	117866255	117866282	AGCTGATCCATGACCAGCCAGTTAGATG
mIFNG-3	10	117865109	117865136	GGATTGTAGTGGCCATTCCTGGTTGTCA
mIFNG-7	10	117860925	117860952	ATAAGACGCAAATTGATGAGAGGGGCAC
mIFNG-8	10	117859977	117860008	GGAAAACATGATGAATGAAAGGAAGGAGTTGT
mIFNG-9	10	117859237	117859264	AGGAGGTAGTGTAGTGGCTATTCCTGGT
mIFNG-11.1	10	117851106	117851136	GCATGGTGACAGAACAGTGGTTCCTAACTTG
mIFNG-12	10	117851105	117851132	TGCATGGTGACAGAACAGTGGTTCCTAA
mIFNG-15	10	117849913	117849940	ATAGCACACAGAAAGGCTGATGCCTCAG
mIFNG-16	10	117847735	117847762	AATACCTATGGAGAGTGTGGGCTCCCTT
mIFNG-17	10	117835003	117835030	AGCAGATTCTGATCCATCAACTCCCACC
mIFNG-19	10	117830081	117830108	AATGGTCACCCTACCAAAAGCAATCAGC
mIFNG-23.1	10	117825733	117825762	AACCCGAACACCATGACTTTTCACAGTATG
mIFNG-24.1	10	117825280	117825308	CAA CTT GGT GAT ATG GGG TTG GTG CAG AG
mActin1	19	34316677	34316704	TAAACTGGCCACTGCTTTCTGATGTCCT
mActin2	19	34319639	34319666	GCGCTAAAATCTACCTGTCCCATGTGAC
mActin3	19	34320562	34320589	CCTCACCAGTAGTCACGAAGGAATAGCC
mActin4	19	34322909	34322936	TTTACCTGGGTCATTTTCTCCCGGTTGG
mActin5	19	34329012	34329039	GATGAAGCTACCGAGCCCTGAGTTACAA
mGDesert1	3	147121450	147121477	AGGGACTGACAGAAGCATCTGGAAACAA
mGDesert2	3	147124499	147124526	AGCCACAAGTTCTCTGAATTTGGTCAAA
mGDesert16	3	147164321	147164348	GCCTAAGAATTATTGGCTCAGTCCAGCA
mGDesert18	3	147170288	147170315	ATGAATCCCACCTGAATGTAAGGCCTGG
mGDesert26	3	147209751	147209780	TGGGTTACTTCACAGACAGATTTTCAAACT
mGAPDH1	6	125113689	125113717	GCTAGTTGAATGCTTGGATGTACAACCCA
mGAPDH2	6	125114192	125114219	AAAAATGAGAGCCGGAGCAACAGATGTG

* MM9 Coordinates
[$] Anchoring Primer